Journal of the Korea Concrete Institute
Vol.17 No.3, pp.481~485, June, 2005

Distribution of Calcium Hydroxide at the ITZ between Steel and Concrete

Ki-Yong Ann[1)]*, Hong-Sam Kim[2)], Yang-Bae Kim[2)], and Han-Young Moon[2)]

[1)] Dept. of Civil and Environmental Engineering, Imperial College, London, UK
[2)] Dept. of Civil Engineering, Hanyang University, Seoul, 133-791, Korea

(Received November 10, 2004, Accepted May 30, 2005)

Abstract

The present study examines the distribution of calcium hydroxide, unhydrated cement grain and porosity at the steel-concrete interface. The formation of calcium hydroxide has been confirmed by microscopic analysis using BSE images containing the ITZ between the steel and concrete. It was found that calcium hydroxide does not form a layer on the steel surface, different from the hypothesis that has been available in investigating the corrosion of steel in concrete, ranging from 5 to 10% within the steel surface. Moreover, the high level of porosity at the ITZ was observed, accounting for 30%, which may reduce the buffering capacity of cement hydration products against a local fall in the pH. These findings may imply that the mole of $[Cl^-]$:$[OH^-]$ in pore solution as chloride threshold level lead to wrong judgement or to a wide range of values.

Keywords: interfacial transition zone, calcium hydroxide, buffering capacity, chloride threshold level

1. Introduction

It is well known that cement hydration products, in particular calcium hydroxide, apart from a ferrous oxide film, have an important role to play as they increase the resistance to a chloride-containing corrosive environment [1,2]. A previous study has postulated that calcium hydroxide forms a layer on the steel surface to protect the embedded steel from corrosion by buffering a local fall in the pH [3]. The level of the pH buffered by calcium hydroxide was later found to be around 12.4[4]. However, this hypothesis has been challenged by Glass et al[5] who observed in backscattered electron (BSE) image that calcium hydroxide does not form a layer at the steel-concrete interface, but its content and distribution has not been quantified.

Despite the importance of the microstructure at the steel-concrete interface that may be influenced by electrochemical treatment, the investigation on the interfacial zone (ITZ) between the steel and concrete has been rarely reported, while the ITZ between the cement matrix and aggregate has been extensively investigated.[6-11]

The present study concerns a quantification of the distribution of calcium hydroxide, porosity and unhydrated cement paste at the ITZ between the steel and the concrete to ensure the generation of calcium hydroxide in the vicinity of the steel. To quantify the distribution of hydration products, BSE images were obtained in the vicinity of the steel and then strips were made 1.5μm in width, up to 100μm away from the steel surface. This method of making strips in the ITZ of interest was previously performed by Scrivener and Gartner.[9] Each strip was extensively analysed to estimate the content of calcium hydroxide, unhydrated cement paste and voids.

2. Experimental works

2.1 Specimen preparation

Mortar specimens were cast with a centrally located steel ribbon (0.25mm thick). The mix proportion for cement: water: sand mixture was 1.00: 0.45: 2.45. The experimental set-up is given in Fig. 1. The mortar was cured for 28 days at room temperature.

* Corresponding author
Email address: ki-yong.ann1@imperial.ac.uk

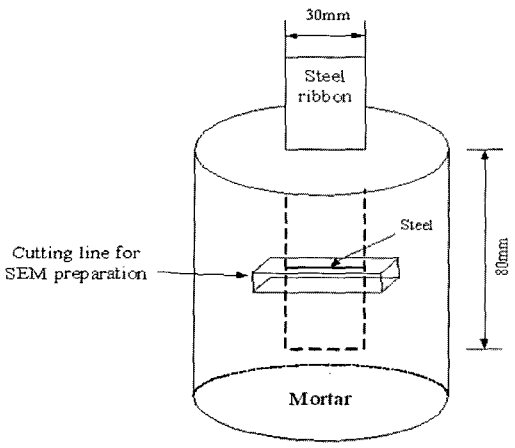

Fig. 1 Experimental set-up for microscopic analysis of the steel-mortar interface

Sample preparation after curing, consists of cutting, drying, vacuum impregnation with resin, lapping, grinding and polishing. Segments containing the steel ribbon were sliced perpendicular to the direction of the steel, using a diamond saw, to produce a block specimen (40 x 20 x 10mm). The specimens were then dried in an oven at 50°C for 3 days and resin impregnated under vacuum. The impregnated specimens were lapped and polished on cloths embedded with diamond particles at five sizes ranging from 9, 6, 3, 1 to 0.25μm. Polishing was performed at 70rpm, with a 7N force applied to each specimen. The time spent on each grinding and polishing stage was no longer than 2-4 minutes to minimise relief effects that may produce an uneven surface due to the different hardness of materials. After polishing, the specimens were cleaned ultrasonically in acetone and then further dried for one day using a vacuum pump at a pressure of the order 10^{-4} Pa, followed by carbon coating under pressure of about 7×10^{-5} Pa. The specimens were stored in a low vacuum cabinet until required for the scanning electron microscopy (SEM) observation. The prepared specimen, as an example, is given in Fig. 2.

2.2 Image capture

A JEOL 5410LV SEM was used for taking BSE images. The instrumental parameters used for the SEM were: accelerating voltage = 20kV; working distance = 15mm; beam spot size (SS) = 12; lens current = 66μA. To avoid an erroneous calculation being introduced by the aggregate, all images were captured at different locations along the steel without the presence of aggregate particles. To ensure random and unbiased sampling, 12 grey scale images were collected per sample at a magnification of 500×. Then, the images obtained were digitised to 1940 × 1455 pixels with a pixel resolution of 0.1237μm; a 500× magnification was

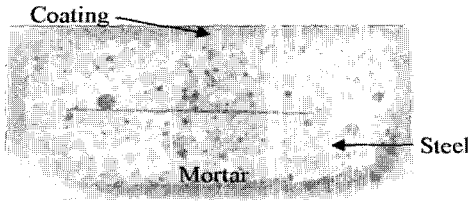

Fig. 2 Example of specimen prepared for BSE image analysis

used to analyse the hydrated cement paste. Areas near the sample edge were not imaged to remove sampling locations that may have been damaged during the digitisation. The image size to evaluate was 1877 × 1430 pixels.

2.3 Quantification of hydration products

To quantify the distribution of calcium hydroxide, porosity and unhydrated cement in the vicinity of the steel surface were determined by (1) binarising images for each phase (2) making narrow strips about 1.48μm wide, extending from the steel surface to 100μm away from the steel and (3) then calculating each phase of interest in a strip.

With binarised image for the steel, strips were produced from the steel-mortar interface at 1.48μm intervals. The total distance to be covered was about 100μm from the steel surface, which requires 67 interface strips. The total area of each strip was measured and then the allocation of calcium hydroxide, porosity and unhydrated cement grains was calculated by image calculation respectively. Fig. 3 gives an example of the BSE image in strips and binarised images of steel, unhydrated cement, calcium hydroxide and porosity.

3. Results

3.1 Histogram

The signal coefficient (η) for each spot is assigned to a grey scale value in the ranged image and can be converted to an image scale with values from 0 to 255. When an image is transferred from the SEM to the image analysis system, pixels with grey levels that represent the signal intensities from corresponding points on the specimen, form the image. There are five major fractions that can be identified at the interface between cement paste and steel using BSE: steel, unhydrated cement, calcium hydroxide, calcium silica hydrate (CSH) gel and porosity. These can be illustrated by a grey scale histogram that represents image pixel data. The cement hydration products identified in the image are labelled at the corresponding histogram peak as shown in Fig. 4. The grey scale in the image depends on the electron density of the material. The phases of interest, graded in terms

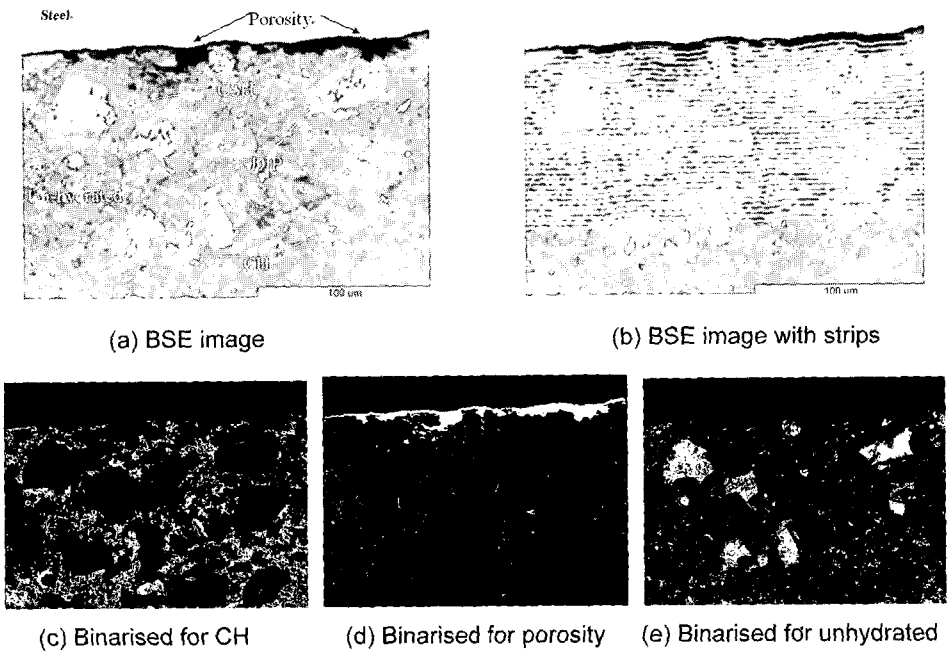

Fig. 3 Image of a specimen containing steel with strips and binarised images for porosity, calcium hydroxide and unhydrated cement

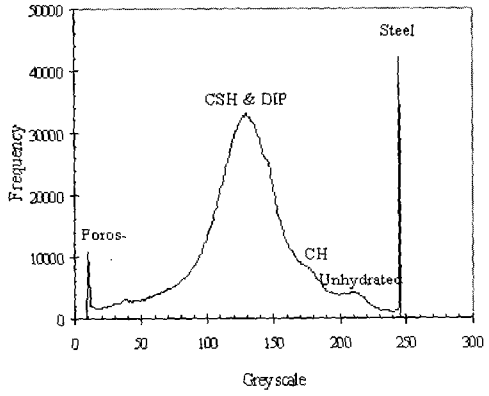

Fig. 4 Histogram for various levels of grey scale

of their brightness (i.e. grey scale), are steel (lightest) > unhydrated cement grains > calcium hydroxide > dense inner product (DIP) and CSH gel > porosity and voids (darkest). After determining the range of grey scale for each phase, the BSE image was binarised to identify each phase. The DIP is often generated surrounding unhydrated cement grains, forming a rim. The content of calcium hydroxide can be overestimated because the grey scale of the DIP is similar to that for calcium hydroxide[6]. To eliminate this error, the rim was manually eliminated in the present study.

3.2 Distribution of hydration products

Figs. 5~7 give the content of porosity, unhydrated cement grain and calcium hydroxide, together with dense inner product (DIP), at the ITZ between the steel and mortar.

The porosity occupying each strip was calculated as a percentage of the total area of the strip. As shown in Fig. 5, the porosity increased significantly within 20μm of the steel. In particular, within 1.5μm of the steel, the porosity accounted for about 30% and then reduced to the much lower values, ranging from 1.68 to 2.88%. This trend of increasing porosity at the steel interface has been also observed on the case of the aggregate-cement paste interface.[6,7,12]

As shown in Fig. 6, the content of unhydrated cement grains was lowest at the interface and increased up to a distance of 30μm from the steel. The unhydrated cement content decreased thereafter, to an average of about 7.55% some 75μm away from the steel.

Fig. 7 shows the distribution of calcium hydroxide according to whether or not taking into account the DIP amount. The difference in the values, induced from the DIP, accounts for 0.33-5.21%, which was not addressed in the present study. Surprisingly, the calcium hydroxide level ranges from only 7.99 to 10.15% at the interface (within 10μm) and from 5.23 to 12.92% within 100μm, which challenges the hypothesis that calcium hydroxide forms a continuous layer on the steel surface.

4. Discussion

BSE image analysis was used to study the influence of electrochemical prevention on the distribution of calcium hydroxide, porosity and unhydrated cement grains at the

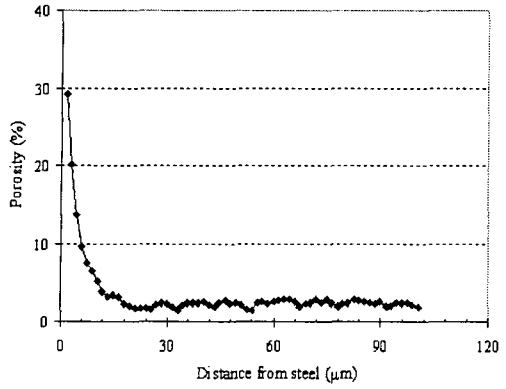

Fig. 5 Distribution of porosity in the vicinity of the steel

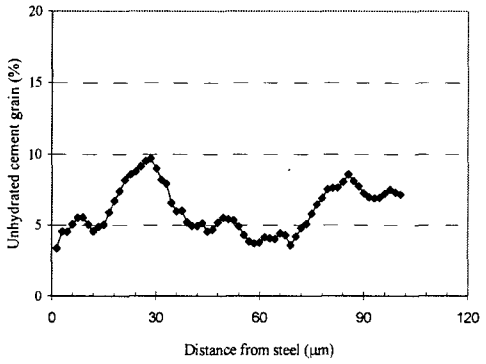

Fig. 6 Distribution of unhydrated cement grain in the vicinity of the steel

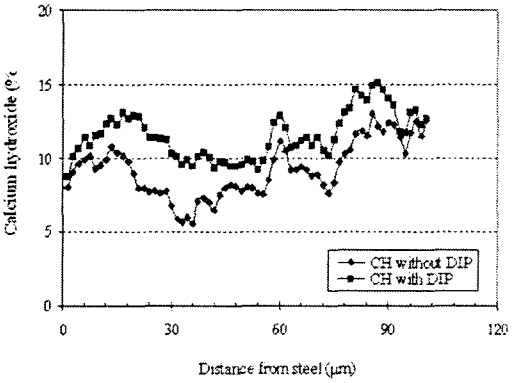

Fig. 7 Distribution of calcium hydroxide, considering the effect of DIP, in the vicinity of the steel

steel-concrete interface, which was quantified in 2 dimensions. Surprisingly, it was found that calcium hydroxide did not form a layer on the steel surface but instead its content increased in the vicinity of the steel. This observation has important implications for determining the chloride threshold level (CTL) for steel corrosion in concrete. It is well known that a precipitated calcium hydroxide layer protects the embedded steel from corrosion by sustaining the alkaline environment at the steel-concrete interface[1, 2, 13, 14], when electrochemical reaction between chloride and ferrous ions forms ferrous chloride followed by ferrous hydroxide, allowing the local pH to fall. Hence, for corrosion to initiate, sufficient amount of chlorides must accumulate at the depth of the steel over the buffering capacity of calcium hydroxide against the pH fall. However, the absence of calcium hydroxide layer suggests that corrosion start at some areas where no protective hydration products are given to the steel. This area for corrosion initiation may be the entrapped air void adjacent to the steel surface. This idea is supported by experimental works showing that corrosion initiates in the air voids generated by bleeding or/and settlement underneath the embedded steel, perpendicular to the direction of concrete casting.[15~17] The importance of the entrapped air void that would otherwise be filled with hydration products also suggests that the CTL is strongly dependent on the interfacial air void content.[18]

Also, the idea of a protective calcium hydroxide layer on the steel has led to the development of tests using a saturated calcium hydroxide solution to determine the CTL expressed as the ratio of $[Cl^-]:[OH^-]$. However, the absence of calcium hydroxide layer allows the pH of pore solution in the vicinity of the embedded steel to be less influencing on corrosion inhibition. The resistance to a local fall in the pH (i.e. acid neutralisation capacity) involves only the area where cement hydration products encompass the steel and thus corrosion initiates in the unprotected area. Previous studies show a wide range of the ratio of $[Cl^-]:[OH^-]$ in similar experimental conditions [19~21], which may be attributed to the absence of the protective layer. A different quantity of calcium hydroxide formed at the steel-concrete interface produces a different level of the buffering capacity to a pH fall and corrosion, which thus may lead to a wide range of $[Cl^-]:[OH^-]$. Hence, the ratio of $[Cl^-]:[OH^-]$, when accompanied by the quantity of cement hydration products at the steel-concrete interface and the interfacial air void content, can be available to express the CTL, which seems however less realistic.

5. Conclusion

The present study examined the distribution of calcium hydroxide, porosity and unhydrated cement paste at the ITZ between the steel and the concrete to ensure the generation of calcium hydroxide. The conclusions of this study are summarised as follows:

1) Microscopic analysis of BSE images containing the steel-concrete interface showed the distribution of the porosity, calcium hydroxide and unhydrated cement grains.

2) Unlike the hypothesis that has been available in the majority of previous studies, precipitated calcium hydroxide does not form a continuous layer on the surface of the embedded steel.
3) Only 5.23-12.92% of calcium hydroxide occupied the ITZ between the steel and the concrete, while the porosity accounted for 30% approximately.

Acknowledgement

This study has been a part of a research project supported by Korea Ministry of Construction and Transportation (MOCT) via the Infra-Structures Assessment Research Center. The authors wish to express their gratitude for the financial support.

References

1. G.K. Glass, B. Reddy, and N.R. Buenfeld, "Corrosion inhibition in concrete arising from its acid neutralisation capacity", *Corrosion Science 42*, 2000, pp.1587~1598.
2. G.K. Glass, B. Reddy, and N.R. Buenfeld, "The participation of bound chloride in passive film breakdown on steel in concrete", *Corrosion Science 42*, 2000, pp.2013~2021.
3. C.L. Page, "Mechanism of corrosion protection in reinforced concrete marine structure", *Nature 256*, 1975, pp.514~515.
4. U. A. Birnin-Yauri and F. P. Glasser, "Friedel's salt, $Ca_2Al(OH)_6(Cl,OH)\cdot 2H_2O$: its solid solutions and their role in chloride binding", *Cement and Concrete Research*, Vol.28, No.12., 1998, pp.1713~1723.
5. G. K. Glass, R. Yang, T. Dickhaus, and N.R. Buenfeld, "Backscattered electron imaging of the steel-concrete interface", *Corrosion Science 43*, 2001, pp.605~610.
6. M. K. Head, *Influence of the interfacial transition zone (ITZ) of properties of concrete*, PhD Thesis, University of Leeds, 2001, pp.63~118.
7. A. R. Brough and A. Atkinson, "Automated identification of the aggregate-paste interfacial transition zone in mortars of silica sand with Portland or alkali-activated slag cement paste", *Cement and Concrete Research*, Vol.30, No.6., 2000, pp.849~854.
8 K. L. Scrivener and K. M. Nemati, "The percolation of pore space in the cement paste/aggregate interfacial zone of concrete", *Cement and Concrete Research*, Vol.26, No.1., 1996, pp.35~40.
9. K. L. Scrivener and E. M. Gartner, "Microstructural gradients in cement paste around aggregate particles, In: Bonding in cementitious composite", *S. Mindness and S.P. Shah eds., Materials Research Society*, Issue 114, 1988, pp.77~86.
10. K. L. Scrivener, A. K. Crumbie, and P. L. Pratt, "A study of the interfacial region between cement paste and aggregate in concrete, In: Bonding in cementitious composite, S. Mindness and S.P. Shah eds.", *Materials Research Society*, Issue 114, 1988, pp.87~88.
11. S. Diamond, "Considerations in image analysis as applied to investigations of the ITZ in concrete", *Cement and Concrete Composites*, Vol.23, No.1., 2001, pp.171~178.
12. K. L. Scrivener and K. M. Nemati, "The percolation of pore space in the cement paste/aggregate interfacial zone of concrete", *Cement and Concrete Research*, Vol26, No.1., 1996, pp.35~40.
13. G. Sergi and G. K. Glass, "A method of ranking the aggressive nature of chloride contaminated concrete", *Corrosion Science 42*, 2000, pp.2043~2049.
14. C. L. Page and K. W. J. Treadaway, "Aspects of the electrochemistry of steel in concrete", *Nature 297*, 1982, pp.109~115.
15. T. U. Mohammed, N. Otsuki, and M. Hisada, "Corrosion of steel bars with respect to orientation of concrete", *ACI Material Journal*, Vol.96, No.2., 1999, pp.154~159.
16. A. Castel, T. Vidal, R. Francois, and G. Arliguie, "Influence of steel-concrete interface quality on reinforcement corrosion induced by chlorides", *Magazine of Concrete Research*, Vol.55, No.2., 2003, pp.151~159.
17. T.A. Soylev and R. Francois, "Quality of steel-concrete interface and corrosion of reinforcing steel", *Cement and Concrete Research*, Vol.33, No.9, 2003, pp.1407~1415.
18. K.Y. Ann, *Enhancing the chloride threshold level for steel corrosion in concrete*, PhD Thesis, University of London, 2005, pp.119~177.
19. V. K. Gouda and W.Y. Halaka, "Corrosion and corrosion inhibition of reinforced steel", *British Corrosion Journal*, Vol.5 , No.2., 1970, pp.204~208.
20. C. Alonso, M. Castellote, and C. Andrade, "Chloride threshold dependence of pitting potential of reinforcements", *Electrochemica Acta 47*, 2002, pp.3469~3481.
21. S. Goni and C. Andrade, "Synthetic concrete pore solution chemistry and rebar corrosion in the presence of chloride", *Cement and Concrete Research*, Vol.20, No.4., 1990, pp.525~539.